

NASA TECHNICAL NOTE



NASA TN D-3694

2.1

LOAN COPY: RETURN TO
AFVWL (WLIL-2)
KIRTLAND AFB, N MEX

0130637

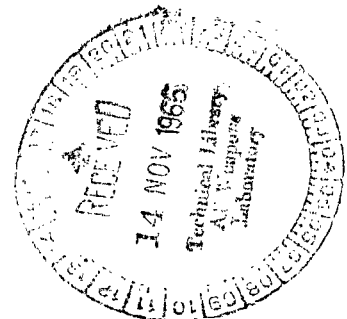


NASA TN D-3694

THE ENERGY REQUIRED TO PRODUCE AN ELECTRON-HOLE PAIR IN SILICON BY TRITONS

by John J. Smithrick and Ira T. Myers

*Lewis Research Center
Cleveland, Ohio*



NATIONAL AERONAUTICS AND SPACE ADMINISTRATION • WASHINGTON, D. C. • OCTOBER 1966



NASA TN D-3694

THE ENERGY REQUIRED TO PRODUCE AN ELECTRON-HOLE
PAIR IN SILICON BY TRITONS

By John J. Smithrick and Ira T. Myers

Lewis Research Center
Cleveland, Ohio

NATIONAL AERONAUTICS AND SPACE ADMINISTRATION

For sale by the Clearinghouse for Federal Scientific and Technical Information
Springfield, Virginia 22151 - Price \$1.00

THE ENERGY REQUIRED TO PRODUCE AN ELECTRON-HOLE PAIR IN SILICON BY TRITONS

by John J. Smithrick and Ira T. Myers

Lewis Research Center

SUMMARY

The energy required to produce an electron-hole pair in silicon by tritons was measured using a sandwich configuration of two silicon surface-barrier detectors with a lithium 6 layer between them. The tritons were generated by the lithium 6 (n, α)triton ($\text{Li}^6(\text{n}, \alpha)\text{T}$) reaction by using thermal neutrons. The measured value of 3.58 ± 0.04 electron volts per electron-hole pair agrees within the experimental error with the energy required to produce an electron-hole pair by alpha particles in silicon.

INTRODUCTION

The energy required to produce an electron-hole pair in a semiconductor is a fundamental quantity in radiation measurements. It must be known in order to calculate the energy deposited in a detector from the ionization collected. In certain types of neutron spectrometers (lithium 6 and helium 3 sandwich-type spectrometers), one semiconductor detector is used to measure one particle energy resulting from a nuclear reaction; a second detector is used to measure the second particle energy, with the two energies (or ionization) being added. For example, the lithium 6 sandwich spectrometer uses the $\text{Li}^6(\text{n}, \alpha)\text{T}$ reaction, and the two detectors measure the recoil energies of the recoil triton and the alpha particle. The sum of the energies of the recoil particles is equal to the incident neutron energy plus the energy Q of the $\text{Li}^6(\text{n}, \alpha)\text{T}$ reaction. Since the Q of the reaction is well known, the neutron energy can be calculated from the sum of the energies of the recoil particles; the sum of recoil particle energies is obtained by an electronic summing process. This energy addition can only be done accurately if the energy per electron-hole pair in silicon is known for both alpha particles and tritons. Considerable experimental information was available for alpha particles but not for tritons. The available theoretical work was not definitive enough to distinguish

between particle types. Since neither experimental nor analytical data were available on the energy required to produce an electron-hole pair in silicon by tritons, an experimental measurement was made with a lithium 6 sandwich-type spectrometer detector and a precision pulse-charge calibrating system.

From energy and momentum relations, the energy shared by the triton and the alpha particle is $E_T = QM_\alpha/(M_\alpha + M_T)$ and $E_\alpha = QM_T/(M_\alpha + M_T)$, respectively. The energy of the triton has to be corrected for the energy spent in the dead layers of the spectrometer detector, gold-layer electrode and the self-shielding of the lithium 6 fluoride (Li^6F) layer. The triton loses a negligible amount of energy in the detector air gap. An analytical determination of the dead layer correction would be difficult due to the problem of accurate calculation of the average dead-layer thickness; hence, an experimental approach was used. In any case, the correction is a small one.

SYMBOLS

C	preamplifier coupling capacitor, (see fig. 6)
$C_{c,c}$	calibration cable capacitance, F
$C_{c,d}$	detector cable capacitance, F
C_d	detector capacitance, F
C_f	preamplifier feedback capacitance, F
C_1, C_2	capacitor, (see fig. 3)
E_T	energy of triton, eV
E'_T	energy of triton corrected for energy loss in dead layers of detector, eV
E_α	energy of alpha particle, eV
e	electronic charge, C
$\left(\frac{dE}{dx}\right)_{T, \text{Au}}$	stopping power of triton in Au, eV/cm
$\left(\frac{dE}{dx}\right)_{T, \text{Li}^6\text{F}}$	stopping power of triton in Li^6F , eV/cm
$\left(\frac{dE}{dx}\right)_{\alpha, \text{Au}}$	stopping power of alpha particle in Au, eV/cm
$\left(\frac{dE}{dx}\right)_{\alpha, \text{Li}^6\text{F}}$	stopping power of alpha particle in Li^6F , eV/cm

G	preamplifier open loop gain
K	average value ratio of stopping power of alpha particle in Au to that of triton in Au and ratio of stopping power of alpha particle in Li^6F to that of triton in Li^6F
M_T	mass of triton, amu
M_α	mass of alpha particle, amu
n	neutron
Q	energy of $\text{Li}^6(n, \alpha)\text{T}$ reaction, 4.78×10^6 eV
q	calibration charge, C
q_c	charge on preamplifier coupling capacitor, C
q_f	charge on preamplifier feedback capacitor, C
q_T	charge deposited in silicon detector by triton, C
q_α	charge deposited in silicon detector by alpha particle, C
R_1, R_2	resistance, ohms (see fig. 3)
V	open circuit potentiometer voltage, V (see fig. 3)
V_b	detector internal bias, V
V_c	voltage across preamplifier coupling capacitor, V
V_d	bias across detector, V
V_f	voltage across feedback capacitor C_f , V (see fig. 6)
V_o	output voltage of amplifier, V (see fig. 6)
\bar{x}_{Au}	average detector Au electrode dead-layer thickness, cm
$\bar{x}_{\text{Li}^6\text{F}}$	average Li^6F dead-layer thickness, cm
ϵ_T	average energy required to produce electron-hole pair in silicon by tritons, eV/electron-hole pair
$\epsilon_{T, m}$	average energy required to produce electron-hole pair in silicon by tritons (uncorrected for detector capacitance loading), eV/electron-hole pair
ϵ_α	average energy required to produce electron-hole pair in silicon by alpha particles, eV/electron-hole pair

DESCRIPTION OF METHOD

In order to measure the triton energy required to produce an electron-hole pair in a material (ϵ_T), it is necessary either to know or measure both the energy lost in the solid and the ionization produced, since ϵ_T is the ratio of these two quantities. In the present work, the tritons from the $\text{Li}^6(n, \alpha)\text{T}$ reaction were used as a source of tritons of known energy, and the charge q_T produced per triton in the silicon was measured with a calibrated amplifier - pulse height analyzer system.

A lithium 6 semiconductor sandwich-type neutron spectrometer detector (ref. 1) was used as a lithium 6 source and also as a detector of tritons and alpha particles. The total energy given the triton and the alpha particle is equal to the neutron energy plus the known Q of the reaction. In this experiment, thermal neutrons were used; hence, the energy given to the triton and the alpha particle was essentially the Q of the reaction.

The derivation of the following equation used to calculate ϵ_T makes use of the known ϵ_α to correct E_T for the energy of a triton in the dead layers of the detector. For tritons,

$$\epsilon_T = \frac{e}{q_T} \left[E_T - \left(\frac{dE}{dx} \right)_{T, \text{Au}} \bar{x}_{\text{Au}} - \left(\frac{dE}{dx} \right)_{T, \text{Li}^6\text{F}} \bar{x}_{\text{Li}^6\text{F}} \right] \quad (1)$$

where

$$\left(\frac{dE}{dx} \right)_{T, \text{Au}} \bar{x}_{\text{Au}}$$

and

$$\left(\frac{dE}{dx} \right)_{T, \text{Li}^6\text{F}} \bar{x}_{\text{Li}^6\text{F}}$$

correspond to the energy lost by a triton in passing through the gold (Au) and Li^6F dead layers, respectively.

Similarly, for alpha particles,

$$\epsilon_{\alpha} = \frac{e}{q_{\alpha}} \left[E_{\alpha} - \left(\frac{dE}{dx} \right)_{\alpha, \text{Au}} \bar{x}_{\text{Au}} - \left(\frac{dE}{dx} \right)_{\alpha, \text{Li}^6\text{F}} \bar{x}_{\text{Li}^6\text{F}} \right] \quad (2)$$

so that

$$E_{\alpha} - \frac{q_{\alpha} \epsilon_{\alpha}}{e} = \left(\frac{dE}{dx} \right)_{\alpha, \text{Au}} \bar{x}_{\text{Au}} + \left(\frac{dE}{dx} \right)_{\alpha, \text{Li}^6\text{F}} \bar{x}_{\text{Li}^6\text{F}} \quad (3)$$

Consider the ratio of the stopping power of an alpha particle in Au to that of triton in Au and the ratio of the stopping power of an alpha particle in Li^6F to that of a triton in Li^6F . From the ratios of the stopping power were obtained equations (4) and (5), with the stopping power values taken from reference 10:

$$\left(\frac{dE}{dx} \right)_{\alpha, \text{Au}} = 3.54 \left(\frac{dE}{dx} \right)_{\text{T}, \text{Au}} \quad (4)$$

$$\left(\frac{dE}{dx} \right)_{\alpha, \text{Li}^6\text{F}} = 5.70 \left(\frac{dE}{dx} \right)_{\text{T}, \text{Li}^6\text{F}} \quad (5)$$

Substituting equations (4) and (5) into equation (3) yields

$$E_{\alpha} - \frac{q_{\alpha} \epsilon_{\alpha}}{e} = 3.54 \left(\frac{dE}{dx} \right)_{\text{T}, \text{Au}} \bar{x}_{\text{Au}} + 5.70 \left(\frac{dE}{dx} \right)_{\text{T}, \text{Li}^6\text{F}} \bar{x}_{\text{Li}^6\text{F}} \quad (6)$$

The average value of 3.54 and 5.70 was designated K. The use of an average value of K as an approximation contributes only a relatively small amount of error to the final results (see table II, p. 10). Factoring K out of the right side of equation (6) yields

$$E_{\alpha} - \frac{q_{\alpha} \epsilon_{\alpha}}{e} = K \left[\left(\frac{dE}{dx} \right)_{\text{T}, \text{Au}} \bar{x}_{\text{Au}} + \left(\frac{dE}{dx} \right)_{\text{T}, \text{Li}^6\text{F}} \bar{x}_{\text{Li}^6\text{F}} \right] \quad (7)$$

so that

$$\frac{1}{K} \left(E_{\alpha} - \frac{q_{\alpha} \epsilon_{\alpha}}{e} \right) = \left(\frac{dE}{dx} \right)_{T, Au} \bar{x}_{Au} + \left(\frac{dE}{dx} \right)_{T, Li^6F} \bar{x}_{Li^6F} \quad (8)$$

Substituting equation (8) into equation (1) gives

$$\epsilon_T = \frac{e}{q_T} \left[E_T - \frac{1}{K} \left(E_{\alpha} - \frac{q_{\alpha} \epsilon_{\alpha}}{e} \right) \right] \quad (9)$$

The use of an average value of K makes it possible to correct for energy loss in the dead layers directly from experimental measurements, rather than having to calculate the corrections.

Let

$$E'_T = E_T - \frac{1}{K} \left(E_{\alpha} - \frac{q_{\alpha} \epsilon_{\alpha}}{e} \right) \quad (10)$$

Substituting equation (10) into equation (9) gives

$$\epsilon_T = \frac{e E'_T}{q_T} \quad (11)$$

where E'_T is the energy of a triton corrected for the energy loss in the Au and the Li^6F dead layers of the spectrometer detector. This correction is necessary since the tritons, because of the dead layers of the detector, do not lose all their energy in the depletion region of the detector. The changes q_T and q_{α} were evaluated experimentally from the average pulse heights of the triton and the alpha particle peaks.

EXPERIMENTAL TECHNIQUE

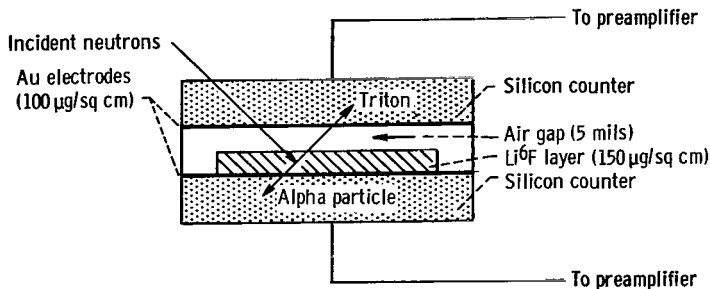


Figure 1. - Neutron spectrometer detector.

A schematic diagram of the lithium 6 spectrometer detector is shown in figure 1. Neutrons incident upon the assembly interact in the Li^6F layer, giving rise to tritons and alpha particles according to the $Li^6(n, \alpha)T$ reaction. The tritons and the alpha particles are detected in

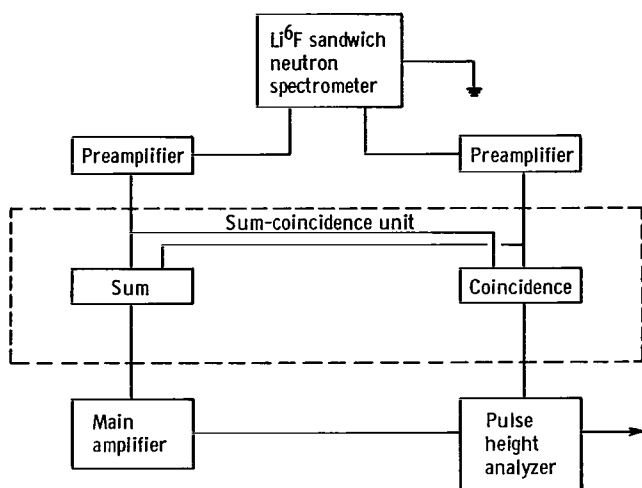


Figure 2. - Neutron spectrometer electronic system.

the two silicon semiconductor counters. The silicon counter pulses are ultimately recorded by a pulse height analyzer. The amplitude of these counter pulses has a one to one correspondence to the triton and the alpha particle energy. The source of thermal neutrons was a 0.5-curie plutonium-beryllium source surrounded by paraffin.

A spectrometer system was used with and without a cadmium cover on the spectrometer detector, and a difference in readings was used to calculate q_T and q_α . The cadmium difference readings were used as weighting factors to calcu-

late the weighted average analyzer pulse height of the triton and the alpha particle. The charge corresponding to the average pulse height of the triton and the alpha particle was then obtained from an analyzer charge calibration curve.

A block diagram of the spectrometer electronic system is shown in figure 2. This system consists of two charge-sensitive preamplifiers, a sum-coincidence unit, a main amplifier, and an 800-channel analyzer (ref. 3). The sum-coincidence unit receives its signals from the two preamplifiers and delivers the sum signal or individual signals from each preamplifier to the main amplifier. If the two signals from the preamplifiers are in time coincidence, they are accepted by the 800-channel pulse height analyzer in response to a gate signal supplied by the sum-coincidence unit. In this experiment, however, the signals were not summed since the interest was in individual triton and alpha particle peaks.

CHARGE CALIBRATION OF ANALYZER

In order to find the charge corresponding to the average triton and alpha particle pulse heights, the analyzer was charge calibrated. This calibration was performed with a mercury-relay precision pulse generator (ref. 4) which was charge terminated for use with a charge-sensitive preamplifier; that is, the pulse generator was terminated in a 100-ohm shunt resistance with a series 1-picofarad 3-terminal capacitor (fig. 3). This capacitor was alternately charged and discharged into a charge-sensitive preamplifier, and the corresponding pulse heights were registered by the analyzer. A schematic representation of the circuit used in this calibration is presented in figure 3.

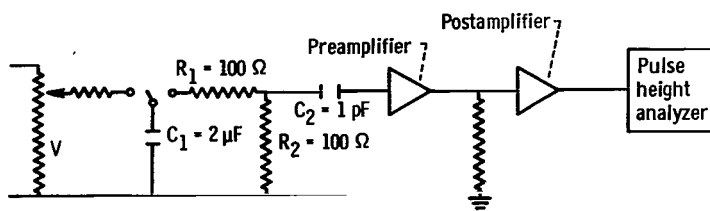


Figure 3. - Diagram of circuit used to charge-calibrate analyzer.

The charge entering the amplifier is given by

$$q = \frac{R_2 C_2 V}{(R_1 + R_2) \left[1 + C_{c,c} \left(\frac{1}{C} + \frac{1}{C_f(G+1)} \right) \right]} \quad (12)$$

Where V is the open circuit voltage of the potentiometer, R_1 , R_2 , and C_2 are defined by the circuit in figure 3. The term $C_{c,c}$ is the capacitance of the calibration cable connecting the capacitor C_2 and the preamplifier input, and C_f and G are the charge-sensitive preamplifier feedback capacitance and the open loop gain, respectively. The bracketed term in equation (12) is a correction for calibration cable capacitance. The effect of cable and leakage capacitances from the junction of R_1 and R_2 to C_2 is negligible (ref. 5). A 0.6 percent correction was also made for charge decay on the capacitor C_1 during pulse integration.

The question has been raised as to whether an appreciable error in the measurement of q was made because of transmission line losses (in particular, to cable capacitance and reflection losses due to mismatching of the transmission line either at the sending or at the receiving end). In an attempt to answer this question, two cables differing in characteristic impedance by a factor of 2 (50- and 100-ohm cables) but of equal total

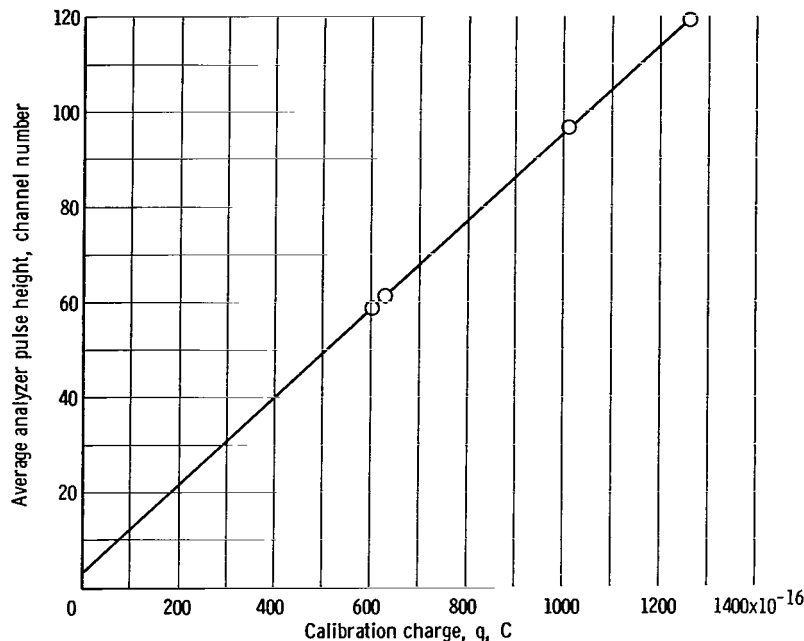


Figure 4. - Average analyzer pulse height as function of calibration charge.

capacitance were employed. The average pulse height ratio was 1.0004. Hence the factor-of-2 difference in characteristic cable impedance makes no appreciable difference in the average pulse height and hence in q . However, changing the total cable capacitance did make a difference in the average pulse height, as expected. The error in the calibration charge q measurement, because of the cable capacitance, was thus corrected.

The analyzer was linear over the voltage range used in the charge calibration. A curve of average analyzer pulse height as a function of the calibration charge is presented in figure 4.

RESULTS AND DISCUSSION

A typical curve of the energy required to produce an electron-hole pair (eV/electron-hole pair) in silicon by tritons as a function of $1/\sqrt{V_d + V_b}$ is presented in figure 5, where V_d is the applied detector bias and V_b is a small internal bias of about 0.6 volt. The dependence of $\epsilon_{T,m}$ (eV/electron-hole pair) on $1/\sqrt{V_d + V_b}$ is due to the capacitance of the detector varying as $1/\sqrt{V_d + V_b}$. The derivation of this dependence and the effect of cable capacitance are given in the appendix.

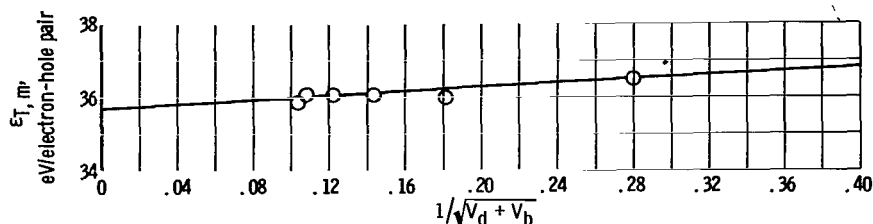


Figure 5. - Typical curve of $\epsilon_{T,m}$ as function of $1/\sqrt{V_d + V_b}$. Detector, 46; diode, 343; ortec channel, B; temperature, 25° C.

TABLE I. - VALUES OF ϵ_T FOR VARIOUS
SPECTROMETER DETECTOR DIODES

Detector	Diode	Ortec channel	ϵ_T , eV/electron-hole pair
46	343	B	3.57
46	343	A	3.55
46	355	A	3.56
48	345	A	3.61
48	359	A	3.60
48	359	A	3.59
Average			3.58±0.04

The $\epsilon_{T,m}$ values extrapolated to infinite detector bias are independent of the applied bias and hence of the capacitance of the detector. Extrapolated values ϵ_T of $\epsilon_{T,m}$ for various detector diodes are presented in table I. All these values agree within the experimental error. Based on the data in this table, the average value of ϵ_T is 3.58 ± 0.04 electron volts per electron-hole pair.

ERROR ANALYSIS

The expression for ϵ_T given by equation (9) is

$$\epsilon_T = \frac{e}{q_T} \left[E_T - \frac{1}{K} \left(E_\alpha - \frac{q_\alpha \epsilon_\alpha}{e} \right) \right]$$

The total error in ϵ_T was taken as the root mean square error (rms) of the systematic and the statistical errors in ϵ_T . The systematic error is due to the uncertainty in the parameters on the right side of equation (13). The statistical error in ϵ_T was computed, based on a 95-percent confidence level, from the standard deviations of the ϵ_T values presented in table I. The total rms error in ϵ_T is 1.2 percent and is based on the data presented in table II.

Table II consists of a list of parameters, their percentage errors, and their rms contribution to the total error in ϵ_T . The data in this table indicate that the systematic error contributes more than the statistical error to the total rms error in ϵ_T , and also

TABLE II. - ROOT MEAN SQUARE CONTRIBUTION TO ERROR IN ϵ_T

[Statistical error, 0.72; total root mean square error, 1.2; ϵ_T , 3.58 ± 0.04 eV/electron-hole pair.]

Parameter	Error in parameter, percent	Root mean square contribution to error in ϵ_T , percent
K	26	0.72
E_T	.48	.49
q_T	.37	.37
ϵ_α	.17	.24
q_α	.56	.094
E_α	.48	.081

that K is the primary contributor to the systematic error. The total rms error in ϵ_T is 1.2 percent.

Based on the information in tables I and II, the average value of ϵ_T is 3.58 ± 0.04 electron volt per electron-hole pair in silicon. A search of literature revealed no other values of ϵ_T . However, $\epsilon_T = 3.58 \pm 0.04$ electron volt per electron-hole pair does agree within the experimental error with $\epsilon_\alpha = 3.56 \pm 0.06$ electron volt per electron-hole pair for an alpha particle in silicon. This average value of ϵ_α was calculated on the basis of the data in table III.

TABLE III. - ENERGY REQUIRED TO
PRODUCE ELECTRON-HOLE PAIR IN
SILICON BY ALPHA PARTICLES

Reference	ϵ_{α} , eV/electron-hole pair
6	3.6 ± 0.3
7	$\left\{ \begin{array}{l} 3.52 \pm 0.04 \\ 3.55 \pm 0.02 \end{array} \right.$
8	3.50 ± 0.05
9	3.61 ± 0.01
Average	3.56 ± 0.06

SUMMARY OF RESULTS

The energy required to produce an electron-hole pair in silicon by tritons was measured using a sandwich configuration of two silicon surface barrier detectors with a lithium 6 layer between them. Irradiation by thermal neutrons gave tritons of known energy, with the resulting pulses measured by a sum-coincidence charge-sensitive amplifier and pulse height analyzer system. The results were

1. The average energy required to produce an electron-hole pair in silicon by tritons is 3.58 ± 0.04 electron volts per electron-hole pair.
2. The average energy required to produce an electron-hole pair in silicon by tritons agrees within the experimental error with that required for alpha particles.

Lewis Research Center,
National Aeronautics and Space Administration,
Cleveland, Ohio, August 18, 1966,
120-27-01-03-22.

APPENDIX - EFFECT OF CIRCUIT AND DETECTOR CAPACITANCE ON CHARGE MEASUREMENTS

A derivation of the equation showing that $\epsilon_{T,m}$ varies as $1/\sqrt{V_d + V_b}$ and showing the effect of cable capacitance is given. As a starting point in this derivation, the circuit diagram presented in figure 6 is considered. An analysis of the circuit presented in figure 6 yields

$$\frac{q_T}{q_f} = \frac{C_d V_d + C_{c,d} V_d + C_f V_f}{C_f V_f} \quad (A1)$$

Since the capacitors C and C_f are in series,

$$q_c = q_f \quad (A2)$$

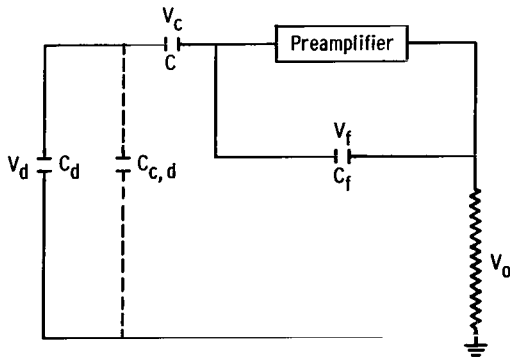
so that

$$C V_c = C_f V_f \quad (A3)$$

Hence,

$$V_c = \frac{C_f V_f}{C} \quad (A4)$$

Furthermore,



$$V_o = \left(\frac{G}{G + 1} \right) V_f \quad (A5)$$

and

$$V_d - V_c = V_f - V_o \quad (A6)$$

$$V_d = V_c + V_f - V_o \quad (A7)$$

Figure 6. - Detector charge-sensitive preamplifier circuit diagram.

Substituting equations (A4) and (A5) into (A7) gives

$$V_d = \frac{C_f V_f}{C} + V_f - \left(\frac{G}{G+1} \right) V_f = V_F \left(\frac{C_f}{C} + \frac{1}{G+1} \right) \quad (A8)$$

Then substituting equation (A8) into equation (A1) yields

$$\frac{q_T}{q_f} = \frac{(C_d + C_{c,d}) \left(\frac{C_f}{C} + \frac{1}{G+1} \right) + C_f}{C_f} \quad (A9)$$

Hence,

$$q_T = q_f \left\{ 1 + C_d \left[\frac{1}{C} + \frac{1}{C_f(G+1)} \right] + C_{c,d} \left[\frac{1}{C} + \frac{1}{C_f(G+1)} \right] \right\} \quad (A10)$$

Substituting equation (A10) into equation (11) yields

$$\epsilon_T = \frac{eE'_T}{q_f \left\{ 1 + C_d \left[\frac{1}{C} + \frac{1}{C_f(G+1)} \right] + C_{c,d} \left[\frac{1}{C} + \frac{1}{C_f(G+1)} \right] \right\}} \quad (A11)$$

Hence,

$$\frac{eE'_T}{q_f} = \epsilon_T \left\{ 1 + C_d \left[\frac{1}{C} + \frac{1}{C_f(G+1)} \right] + C_{c,d} \left[\frac{1}{C} + \frac{1}{C_f(G+1)} \right] \right\} \quad (A12)$$

Now, dividing equation (A12) by $1 + C_{c,d} \left[\frac{1}{C} + \frac{1}{C_f(G+1)} \right]$ gives

$$\frac{eE'_T}{q_f \left\{ 1 + C_{c,d} \left[\frac{1}{C} + \frac{1}{C_f(G+1)} \right] \right\}} = \epsilon_T \frac{1 + C_d \left[\frac{1}{C} + \frac{1}{C_f(G+1)} \right] + C_{c,d} \left[\frac{1}{C} + \frac{1}{C_f(G+1)} \right]}{1 + C_{c,d} \left[\frac{1}{C} + \frac{1}{C_f(G+1)} \right]} \quad (A13)$$

Now $\epsilon_{T,m}$ is defined as equivalent to the left side of equation (A13) so that

$$\epsilon_{T,m} = \epsilon_T \frac{1 + C_d \left[\frac{1}{C} + \frac{1}{C_f(G+1)} \right] + C_{c,d} \left[\frac{1}{C} + \frac{1}{C_f(G+1)} \right]}{1 + C_{c,d} \left[\frac{1}{C} + \frac{1}{C_f(G+1)} \right]}$$

Equation (A13) shows that $\epsilon_{T,m}$ varies as $1/\sqrt{V_d + V_b}$, since $C_d \propto 1/\sqrt{V_d + V_b}$, in agreement with the experimental curve of figure 5. The reason for defining $\epsilon_{T,m}$ is that in the limit as $V \rightarrow \infty$, $\epsilon_{T,m} = \epsilon_T$ because the limit of $c_d = 0$ as $V \rightarrow \infty$.

REFERENCES

1. Anon.: Instruction Manual for Surface Barrier Detectors. Oak Ridge Technical Enterprises Corporation, Oak Ridge, Tennessee.
2. Whyte, George N.: Principles of Radiation Dosimetry. John Wiley and Sons, Inc., 1959.
3. Anon.: Instruction Manual for ORTEC Model 102 Sum Coincidence Unit. Oak Ridge Technical Enterprises Corporation, Oak Ridge, Tennessee.
4. Anon.: Instruction Manual for ORTEC Model 204 Precision Pulse Generator. Oak Ridge Technical Enterprises Corporation, Oak Ridge, Tennessee.
5. Emery, F. E.; and Rabson, T. A.: On the Accuracy of the Calibration Technique Used With Semiconductor Detectors. Nuc. Instr. Methods, vol. 34, 1965, pp. 171-172.
6. McKay, K. G.; and McAfee, K. B.: Electron Multiplication in Silicon and Germanium. Phys. Rev., vol. 91, no. 5, Sept. 1953, pp. 1079-1084.
7. Baldinger, E.; Czaja, W.; and Gutmann, J.: Eine Genaue Bestimmung der Arbeit Pro Electron-Loch-Paar in Si-Zähldioden. Helv. Phys. Acta, vol. 35, no. 7/8 1962, pp. 559-560.
8. Halbert, M. L.; and Blankenship, J. L.: Response of Semiconductor Surface-Barrier Counters to Nitrogen Ions and Alpha Particles. Nuc. Inst. Methods, vol. 8, 1960, pp. 106-116.
9. Bussolati, C.; Fiorentini, A.; and Fabri, G.: Energy for Electron-Hole Pair Generation in Silicon by Electrons and α Particles. Phys. Rev., vol. 136, no. 6A, Dec. 1964, pp. A1756-1758.
10. Williamson, C.; and Boujot, J. P.: Tables of Range and Rate of Energy Loss of Charged Particles of Energy 0.5 to 150 MeV. Rept. No. CEA 2189, Commissariat à l'Énergie Atomique, Centre d'Etudes Nucléaires, Saclay, France, 1962.

"The aeronautical and space activities of the United States shall be conducted so as to contribute . . . to the expansion of human knowledge of phenomena in the atmosphere and space. The Administration shall provide for the widest practicable and appropriate dissemination of information concerning its activities and the results thereof."

—NATIONAL AERONAUTICS AND SPACE ACT OF 1958

NASA SCIENTIFIC AND TECHNICAL PUBLICATIONS

TECHNICAL REPORTS: Scientific and technical information considered important, complete, and a lasting contribution to existing knowledge.

TECHNICAL NOTES: Information less broad in scope but nevertheless of importance as a contribution to existing knowledge.

TECHNICAL MEMORANDUMS: Information receiving limited distribution because of preliminary data, security classification, or other reasons.

CONTRACTOR REPORTS: Technical information generated in connection with a NASA contract or grant and released under NASA auspices.

TECHNICAL TRANSLATIONS: Information published in a foreign language considered to merit NASA distribution in English.

TECHNICAL REPRINTS: Information derived from NASA activities and initially published in the form of journal articles.

SPECIAL PUBLICATIONS: Information derived from or of value to NASA activities but not necessarily reporting the results of individual NASA-programmed scientific efforts. Publications include conference proceedings, monographs, data compilations, handbooks, sourcebooks, and special bibliographies.

Details on the availability of these publications may be obtained from:

SCIENTIFIC AND TECHNICAL INFORMATION DIVISION
NATIONAL AERONAUTICS AND SPACE ADMINISTRATION

Washington, D.C. 20546